Acta Crystallographica Section C
Crystal Structure Communications
ISSN 0108-2701

Lithium barium silicate, Li_2BaSiO_4, from synchrotron powder data

Jinyoung Kim,[a] Docheon Ahn,[b] Chandramouli Kulshreshtha,[c] Kee-Sun Sohn[c] and Namsoo Shin[b]*

[a]Department of Materials Science and Engineering, Pohang University of Science and Technology, Pohang 790-784, Republic of Korea, [b]Pohang Accelerator Laboratory, Pohang University of Science and Technology, Pohang 790-784, Republic of Korea, and [c]Department of Materials Science and Metallurgical Engineering, Sunchon National University, Chonam 540-742, Republic of Korea
Correspondence e-mail: sns@postech.ac.kr

Received 12 January 2009
Accepted 19 February 2009
Online 7 March 2009

The structure of lithium barium silicate, Li_2BaSiO_4, has been determined from synchrotron radiation powder data. The title compound was synthesized by high-temperature solid-state reaction and crystallizes in the hexagonal space group $P6_3cm$. It contains two Li atoms, one Ba atom (both site symmetry ..*m* on special position 6*c*), two Si atoms [on special positions 4*b* (site symmetry 3..) and 2*a* (site symmetry 3.*m*)] and four O atoms (one on general position 12*d*, and three on special positions 6*c*, 4*b* and 2*a*). The basic units of the structure are $(Li_6SiO_{13})^{5-}$ units, each comprising seven tetrahedra sharing edges and vertices. These basic units are connected by sharing corners parallel to [001] and through sharing $(SiO_4)^{4-}$ tetrahedra in (001). The relationship between the structures and luminescence properties of Li_2SrSiO_4, Li_2CaSiO_4 and the title compound is discussed.

Comment

There are several ways of constituting white light based on the LED technique, each of which involves various phosphors, which emit visible light by absorbing soft UV or blue light produced by LEDs. The representative oxide phosphors are $Y_3Al_5O_{12}:Ce^{3+}$ (YAG) and its variants, and divalent europium-doped orthosilicates. As a result of their potential for use as white LEDs, Li_2SrSiO_4 (LSSO), Li_2CaSiO_4 (LCSO) and Li_2BaSiO_4 (LBSO) have recently been reported (Toda *et al.*, 2006). In the present study, the structure of LBSO was determined and refined from synchrotron powder diffraction data (Fig. 1). The structure consists of two types of tetrahedra, *viz.* $(SiO_4)^{4-}$ and $(LiO_4)^{7-}$, with Ba^{2+} atoms located at the centers of open spaces formed by the tetrahedra (Fig. 2). These tetrahedra share edges to form $(Li_6SiO_{13})^{5-}$ units, each comprising seven tetrahedra. The units are connected by sharing corners (O atoms) parallel to [001] and through sharing $(SiO_4)^{4-}$ tetrahedra in (001) (Fig. 3). The bond-valence sum (Brese & O'Keeffe, 1991) of the Ba^{2+} ion is close to the ideal value [S = 1.95 valence units (v.u.)]. The $Si2^{4+}$, $Li1^{1+}$ and $Li2^{1+}$ ions also reveal ideal bond-valence sums (S = 3.99, 1.02 and 0.99 v.u., respectively), while the bond-valence sum of the $Si1^{4+}$ ion (S = 3.62 v.u.) deviates from the ideal value. This deviation is due to the longer bond length between atoms Si1 and O4 compared with those with the three O2 atoms (Table 1). Atom O4 is common to the Li1, Li2 and Si1 tetrahedra. Because of the Li—O interactions, the $(SiO_4)^{4-}$ tetrahedron is distorted and the $Si1^{4+}$ ion is underbonded.

The structures of LSSO ($P3_121$; isostructural with Li_2EuSiO_4; Haferkorn & Meyer, 1998) and LCSO ($I\bar{4}2m$; Gard & West, 1973) also consist of $(SiO_4)^{4-}$ and $(LiO_4)^{7-}$ tetrahedra sharing edges; however, these tetrahedra do not form a compact $(Li_6SiO_{13})^{5-}$ unit as in the title compound.

When LSSO, LCSO and LBSO serve as phosphors, activator ions, such as Eu^{2+} in the present case, have to occupy the

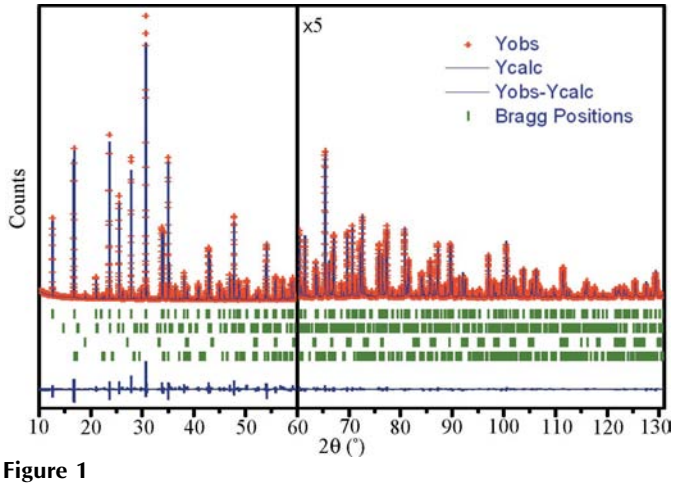

Figure 1
A comparison between the observed and calculated diffraction patterns, and the difference curve.

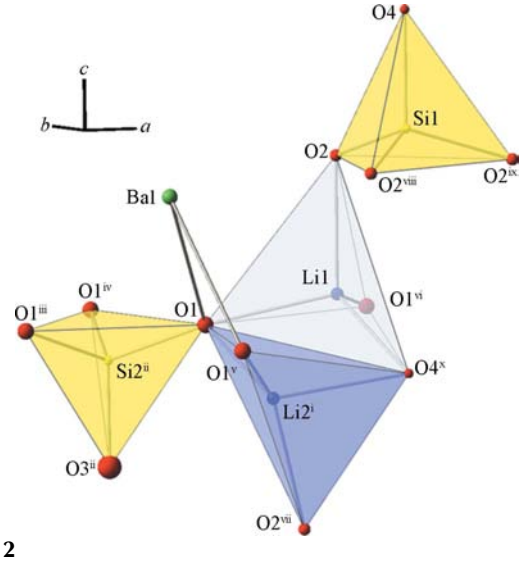

Figure 2
A view of the asymmetric unit and some symmetry-related atoms of the title compound. [Symmetry code: (i) $y, x, z-1$; (ii) $x, x-y, z-\frac{1}{2}$; (iii) $y-x+1, -x+1, z$; (iv) $-y+1, x-y, z$; (v) $x-y, -y, z$; (vi) $-x+1, y-x+1, z$; (vii) $-y+1, x, z-\frac{1}{2}$; (viii) $-y+1, -y, z$; (ix) $y+1, x, z$; (x) $-x, -y, z-\frac{1}{2}$.]

alkaline earth sites. In this regard, the local structure around the alkaline earth site has a great influence on the luminescent behavior. Dorenbos (2000*a*, 2000*b*, 2003) summarized the crystal field splitting in various Ce^{3+}-doped phosphors and suggested a systematic model that describes the crystal field splitting in terms of polyhedron shape and ligand distance. Dorenbos (2003) also found that the centroid shift, crystal field splitting, red shift and Stokes shift values for Eu^{2+} ions can be predicted from those measured for Ce^{3+} ions. The crystal field splitting is proportional to $1/R_{\rm eff}^2$, with a constant designating the polyhedral shape, where $R_{\rm eff}$ is the effective average ligand distance. The Sr, Ca and Ba polyhedra in LSSO, LCSO and LBSO have site symmetries 2, $\bar{4}2m$ and m, respectively, and different coordination numbers. Measured crystal field splittings of LSSO, LCSO and LBSO phosphors (Kulshreshtha, Sharma & Sohn, 2009) show that higher symmetry, smaller coordination number and larger polyhedron size (ligand distance) lead to greater crystal field splitting.

On the other hand, the centroid shift is proportional to $N\alpha_{sp}/R_{\rm eff}^6$ according to the ligand polarization model, where N is the coordination number and α_{sp} is the anion polarizability of the nearest anion neighbors (Dorenbos, 2000*a*, 2000*b*). Using experimentally measured centroid shift and ligand distance data for LSSO, LCSO and LBSO (Kulshreshtha, Sharma & Sohn, 2009), we confirmed that the greater the cation size, the higher the polarizability.

The energy transfer among the Eu^{2+} ions located at the alkaline earth site is also affected significantly by the local structure around the site. The angular class model proposed by Vasquez (1996) was found to be in a good agreement with the energy transfer rate obtained from the decay measurement for LSSO, LCSO and LBSO phosphors (Kulshreshtha, Shin & Sohn, 2009). The site-symmetry information was incorporated into the model *via* several parameters, such as position-generating vector of an angular class, maximum number of activators in an angular class and Riemann's zeta function of dipole–dipole interaction. It was found that the higher the site symmetry of the activator sites, the higher the energy transfer rate.

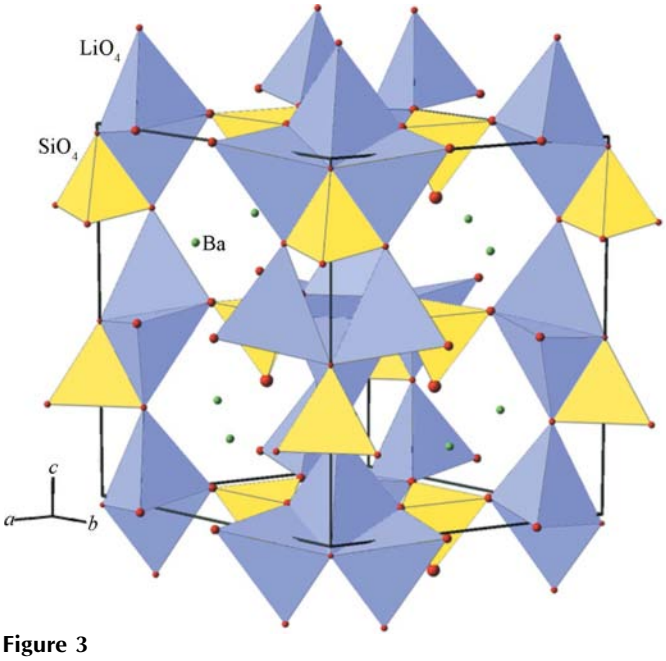

Figure 3
The structure of Li_2BaSiO_4. Ba atoms (green spheres in the electronic version of the paper), [SiO_4] tetrahedra (yellow) and [LiO_4] tetrahedra (blue) are shown.

Experimental

LBSO was synthesized by a high-temperature solid-state reaction using stoichiometric quantities of high purity oxides, namely lithium carbonate (Li_2CO_3, Sigma Aldrich, 99.99%), barium carbonate ($BaCO_3$, Kojundo Chemicals Ltd, 99.9%) and silicon oxide (SiO_2, Kojundo Chemical Ltd, 99.9%). A stoichiometric mixture was weighed and mixed thoroughly in an agate mortar with the addition of acetone; the mixture was then triturated several times for homogenization. The preparation was subsequently placed in alumina crucibles and preheated in air at 573 K for 3 h, then ground again and heated at 1123 K under a reducing atmosphere of a 25%H_2–75%N_2 stream in a horizontal tube furnace for 16 h, so that the desired oxidation state of the activator ion could be attained. After firing, the samples were cooled to achieve room temperature in the furnace and were ground again with an agate mortar for further use. Small amounts of Ba_2SiO_4, Li_2SiO_3 and Li_4SiO_4 were detected as impurities.

Crystal data

Li_2BaSiO_4
M_r = 243.3
Hexagonal, $P6_3cm$
a = 8.10040 (1) Å
c = 10.60052 (1) Å
V = 602.38 (1) Å^3
Z = 6
Synchrotron radiation
λ = 1.54960 Å
T = 298 K
Specimen shape: flat sheet
20 × 0.5 mm
Specimen prepared at 1123 K
Powder, white

Data collection

Pohang Light Source 8C2 HRPD beamline
Specimen mounting: packed powder pellet
Specimen mounted in reflection mode
Scan method: step
$2\theta_{\rm min}$ = 10, $2\theta_{\rm max}$ = 131°
Increment in 2θ = 0.01°

Refinement

$R_{\rm p}$ = 0.090
$R_{\rm wp}$ = 0.121
$R_{\rm exp}$ = 0.072
$R_{\rm B}$ = 0.037
S = 1.70
Excluded region(s): none
Profile function: pseudo-Voigt
50 parameters
Preferred orientation correction: none

Table 1
Selected bond lengths (Å).

Ba1—O1	2.713 (10)	Li1—O1	1.989 (5)
Ba1—O3	2.631 (6)	Li1—O2	2.036 (11)
Si1—O2	1.644 (6)	Li1—O4$^{\rm xiii}$	1.885 (12)
Si1—O4$^{\rm xi}$	1.73 (2)	Li2—O1$^{\rm xiv}$	1.963 (5)
Si2—O1$^{\rm xii}$	1.635 (6)	Li2—O2$^{\rm xv}$	1.985 (10)
Si2—O3	1.596 (16)	Li2—O4$^{\rm xvi}$	2.023 (3)

Symmetry codes: (xi) $x+1, y, z$; (xii) $x, x-y, z+\frac{1}{2}$; (xiii) $x-y+1, x, z-\frac{1}{2}$; (xiv) $-y, x-y, z+1$; (xv) $-x+1, -y+1, z+\frac{1}{2}$; (xvi) $x-y, x+1, z+\frac{1}{2}$.

The diffraction pattern also includes peaks from Ba_2SiO_4 (*Pmcn*, a = 5.8115 Å, b = 10.2135 Å and c = 7.5035 Å), Li_2SiO_3 (*Cmc*2$_1$, a =

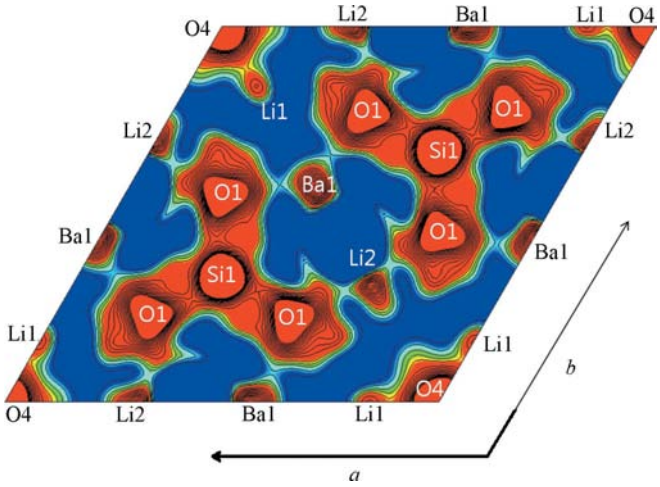

Figure 4
The charge density map obtained by the maximum entropy method in the (001) plane at z = 0.06.

9.4008 Å, b = 5.4073 Å and c = 4.6529 Å) and Li_4SiO_4 ($P2_1/m$, a = 5.1469 Å, b = 6.1051 Å, c = 5.2960 Å and β = 90.3546°) (ICSD, 2008), but the peaks of Li_2BaSiO_4 and those of the impurities are well separated from one another in the high-resolution synchrotron radiation powder pattern, at least in the low and medium scattering angle region. We could easily exclude the peaks of impurities from the peaks used for unit-cell determination. The Li_2BaSiO_4 powder diffraction pattern was indexed in the hexagonal system using *TREOR* (Werner *et al.*, 1985) with figure of merit $M30$ = 271.0 ($F30$ = 448.0). The 2θ difference between the positions of observed and calculated peaks was less than 0.002°. The space group $P6_3cm$ (No. 185) was chosen from the systematic absences and confirmed by the subsequent structure refinement. The positions of Ba and Si atoms were determined by direct methods using the integrated intensities in the *FULLPROF* suite (Rodriguez-Carvajal, 1990). The positions of O atoms were determined by the simulated annealing method in *FULLPROF*. The positions of Li atoms were determined by the maximum entropy method using the *ENIGMA* package (Sakata & Sato, 1990). Fig. 4 shows the positions of Li atoms on the plane with z = 0.06. The Rietveld refinement was initiated using the aggregate atomic positions obtained from the direct, simulated annealing and maximum entropy methods.

Data collection: PLS HRPD beamline software; cell refinement: *FULLPROF* (Rodriguez-Carvajal, 1990); data reduction: *FULLPROF*; program(s) used to solve structure: *FULLPROF* and *ENIGMA* (Sakata & Sato, 1990); program(s) used to refine structure: *FULLPROF*; molecular graphics: *Balls&Sticks* (Ozawa & Kang, 2004); software used to prepare material for publication: *FULLPROF*.

This work was supported by the Ministry of Knowledge Economy (MKE) through the Regional Innovation Center (RIC). The experiment at PLS was supported in part by MOST and POSTECH.

Supplementary data for this paper are available from the IUCr electronic archives (Reference: SQ3185). Services for accessing these data are described at the back of the journal.

References

Brese, N. E. & O'Keeffe, M. (1991). *Acta Cryst.* B**47**, 192–197.
Dorenbos, P. (2000*a*). *Phys. Rev. B*, **62**, 15640–15649.
Dorenbos, P. (2000*b*). *Phys. Rev. B*, **62**, 15650–15659.
Dorenbos, P. (2003). *J. Phys. Condens. Matter*, **15**, 4797–4807.
Gard, J. A. & West, A. R. (1973). *J. Solid State Chem.* **7**, 422–427.
Haferkorn, B. & Meyer, G. (1998). *Z. Anorg. Allg. Chem.* **624**, 1079–1081.
ICSD (2008). Inorganic Crystal Structure Database. FIZ Karlsruhe, Germany, and Gmelin Institut, Frankfurt, Germany.
Kulshreshtha, C., Sharma, A. K. & Sohn, K.-S. (2009). *J. Electrochem. Soc.* **156**, J52–56.
Kulshreshtha, C., Shin, N. & Sohn, K.-S. (2009). *Electrochem. Solid State Lett.* In the press.
Ozawa, T. C. & Kang, S. J. (2004). *J. Appl. Cryst.* **37**, 679.
Rodriguez-Carvajal, J. (1990). Abstracts of the Satellite Meeting on Powder Diffraction of the XV Congress of the IUCr, p. 127, Toulouse, France.
Sakata, M. & Sato, M. (1990). *Acta Cryst.* A**46**, 263–270.
Toda, K., Kawakami, Y., Kousaka, S., Ito, Y., Komenno, A., Uematsu, K. & Sato, M. (2006). *IEICE Trans. Electron.* **E89–C**, 1406–1412.
Vasquez, S. O. (1996). *J. Chem. Phys.* **104**, 7652–7657.
Werner, P.-E., Eriksson, L. & Westdahl, M. (1985). *J. Appl. Cryst.* **18**, 367–370.